Journal of Solid State Chemistry **164,** 98–105 (2002)
doi:10.1006/jssc.2001.9452, available online at http://www.idealibrary.com on IDEAL®

Structural Characterization of the Complex Perovskites $Ba_{1-x}La_xTi_{1-x}Cr_xO_3$

Guobao Li,†,[1] Yoshiaki Uesu,* and Kay Kohn*

*Department of Physics, Waseda University, 3-4-1 Okubo, Shinjuku-ku, Tokyo 169-8555, Japan; and †College of Chemistry and Molecular Engineering, Peking University, Beijing 100871, China

Received August 7, 2001; in revised form October 25, 2001; accepted November 12, 2001

The series $Ba_{1-x}La_xTi_{1-x}Cr_xO_3$ ($0 \le x \le 1$) was synthesized at 1400°C for about 60 h. Their structure was carefully analyzed by the use of powder X-ray diffraction and Rietveld analysis software GSAS (General Structure Analysis System). Four solid solutions are found in this series: tetragonal solid solution $Ba_{1-x}La_xTi_{1-x}Cr_xO_3$ ($0 \le x \le 0.029$), cubic solid solution $Ba_{1-x}La_xTi_{1-x}Cr_xO_3$ ($0.0365 \le x \le 0.600$), rhombohedral solid solution $Ba_{1-x}La_xTi_{1-x}Cr_xO_3$ ($0.700 \le x \le 0.873$), and orthorhombic solid solution $Ba_{1-x}La_xTi_{1-x}Cr_xO_3$ ($0.956 \le x \le 1$). There are corresponding two-phase regions between the adjacent two solid solutions. The detailed lattice parameters are presented. The relationship between the lattice parameters and the composition of the solid solutions is developed.

1. INTRODUCTION

To build up a healthy environment, lead-free relaxors have been the subject of intense research. Many doped materials were reported to show relaxor behavior, such as solid solutions of doped $BaTiO_3$ (1–9), doped $SrTiO_3$ (9–19), and doped $KTaO_3$ and $KNbO_3$ (20–25). However, the relaxor behavior occurred at a temperature far from room temperature for most of the above materials. A room-temperature lead-free relaxor is still unknown.

In order to find a new room-temperature lead-free relaxor, the series $Ba_{1-x}La_xTi_{1-x}Cr_xO_3$ was synthesized and characterized. Room-temperature relaxor-like behavior is found in this series and has been reported elsewhere (26), which is very similar to the results reported by Li and Subramanian (27). Here, detailed structure information is presented.

2. EXPERIMENTAL

The series $Ba_{1-x}La_xTi_{1-x}Cr_xO_3$ ($x = 0$, 0.003, 0.006, 0.010, 0.014, 0.018, 0.022, 0.025, 0.028, 0.030, 0.035, 0.04, 0.05, 0.06, 0.08, 0.10, 0.20, 0.40, 0.50, 0.52, 0.54, 0.56, 0.58, 0.60, 0.62, 0.64, 0.66, 0.68, 0.70, 0.74, 0.78, 0.80, 0.82, 0.84, 0.86, 0.88, 0.90, 0.93, 0.94, 0.95, 0.96, 0.97, 0.98, 1.0, named as BLTC01, BLTC02, …, BLTC44) has been synthesized from stoichiometric amounts of La_2O_3, $BaCO_3$, Cr_2O_3, and TiO_2 (high-purity grade). The oven-dried reactants were mixed and homogenized by grinding for about 30 min a total of 6 g of the mixtures in an agate mortar. The mixtures underwent 18 h of heat treatment at 1300°C with three intermediate grinding steps. They were then pressed into pellets to undergo 10 h of heat treatments at 1400°C six times, followed by a furnace cooling every time with intermediate grinding and pressing into pellets. All the treatments were done in air. The weights of the samples were monitored before and after heat treatments. The maximum difference was about 4 mg for the 6-g samples. Therefore, the final compositions of the samples were considered the same as the initial ones.

X-ray diffraction data of the samples were obtained with a RINT diffractometer employing Fe $K\alpha$ radiation ($\lambda_{K\alpha1} = 1.93604$ Å, $\lambda_{K\alpha2} = 1.93998$ Å), Mn filter, 40 kV, 20 mA, and a step scanning method with $\Delta 2\theta = 0.02°$, $\Delta t = 6$ s. The scanning 2θ range is 24° to 150°.

The X-ray diffraction data were analyzed using GSAS software to obtain the lattice parameters. Acceptable fittings between the experimental data and the proposed models have been obtained with $R_p < 4.0\%$, $R_{wp} < 5.0\%$ for all data.

3. RESULTS AND DISCUSSION

The series $Ba_{1-x}La_xTi_{1-x}Cr_xO_3$ ($0 \le x \le 1$) is very complex. It has been found that there exist in this series four different solid solutions: tetragonal solid solution, cubic solid solution, rhombohedral solid solution, and orthorhombic solid solution. Figure 1 shows the change of the volume per ABO_3 molecule of these four solid solutions. Between every two adjacent solid solution, there is a gap, a two-phase area.

[1]To whom correspondence should be addressed. E-mail: gblicn@263.net.

0022-4596/02 $35.00

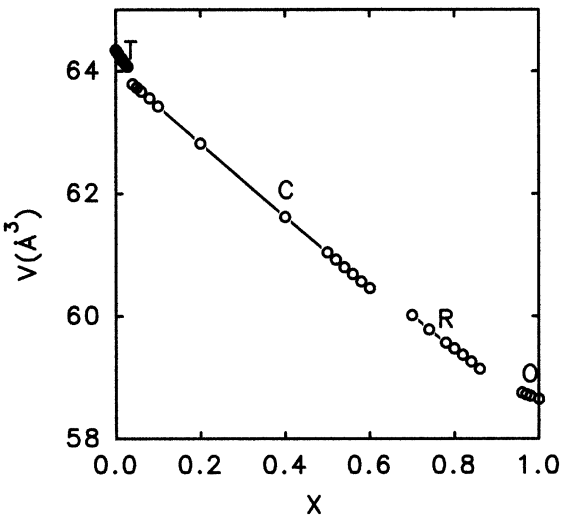

FIG. 1. Dependence on x of the volume per ABO_3 molecule of the four solid solutions in the series $Ba_{1-x}La_xTi_{1-x}Cr_xO_3$ ($0 \le x \le 1$): T, tetragonal solid solution $Ba_{1-x}La_xTi_{1-x}Cr_xO_3$ ($0 \le x \le 0.029$); C, cubic solid solution $Ba_{1-x}La_xTi_{1-x}Cr_xO_3$ ($0.0365 \le x \le 0.600$); R, rhombohedral solid solution $Ba_{1-x}La_xTi_{1-x}Cr_xO_3$ ($0.700 \le x \le 0.873$); O, orthorhombic solid solution $Ba_{1-x}La_xTi_{1-x}Cr_xO_3$ ($0.956 \le x \le 1$).

TABLE 1
Lattice Parameters a and c of the Tetragonal Phase in the Series $Ba_{1-x}La_xTi_{1-x}Cr_xO_3$

Sample	x	a (Å)	c (Å)
BLTC01	0.000	3.9934(1)	4.0348(1)
BLTC02	0.003	3.9934(1)	4.0328(1)
BLTC03	0.006	3.9941(1)	4.0294(1)
BLTC04	0.010	3.9944(1)	4.0258(1)
BLTC05	0.014	3.9952(1)	4.0226(1)
BLTC06	0.018	3.9955(1)	4.0189(1)
BLTC07	0.022	3.9961(1)	4.0156(1)
BLTC08	0.025	3.9964(1)	4.0133(1)
BLTC09	0.028	3.9968(1)	4.0109(1)
BLTC10	0.030	3.9969(1)	4.0096(1)
BLTC11	0.035	3.9969(1)	4.0096(1)

3.1. Tetragonal Solid Solution

It is well known that at room temperature $BaTiO_3$ is of tetragonal symmetry (28–30), called t-$BaTiO_3$. The space group for it is *P*4*mm*. In general, when a small amount of the doping agents is added into $BaTiO_3$, a tetragonal solid solution always forms. This is also true under the present conditions. The samples BLTC02, BLTC03, …, BLTC09 (corresponding to $Ba_{1-x}La_xTi_{1-x}Cr_xO_3$ with $x = 0.003$, 0.006, 0.010, 0.014, 0.018, 0.022, 0.025, 0.028) are found to be single-phase samples with the same structure as t-$BaTiO_3$. The corresponding lattice parameters are listed in Table 1. Figure 2 shows the typical powder X-ray diffraction pattern of the sample BLTC05 with the GSAS fit.

The change of the lattice parameters a and c with increasing doping fulfilled Vegard's law (31, 32), as shown in Fig. 3:

$$a_{tx} = a_{t0}(1 - x) + a_{t1}x \qquad [1]$$

$$c_{tx} = c_{t0}(1 - x) + c_{t1}x. \qquad [2]$$

Here a_{tx}, a_{t0}, a_{t1} and c_{tx}, c_{t0}, c_{t1} are the lattice parameters a and c of tetragonal $Ba_{1-x}La_xTi_{1-x}Cr_xO_3$, pure tetragonal $BaTiO_3$, and the supposed tetragonal $LaCrO_3$; x is the ratio of La/(La + Ba) in $Ba_{1-x}La_xTi_{1-x}Cr_xO_3$. The data fitted the above equation very well with $a_{t0} = 3.9932$ Å, $c_{t0} = 4.0348$ Å for tetragonal $BaTiO_3$ and $a_{t1} = 4.1217$ Å, $c_{t1} = 3.1707$ Å for the supposed tetragonal $LaCrO_3$. The expected a and c ($a_{t0}$and c_{t0}) for the tetragonal $BaTiO_3$ agreed well with the experimental data $a = 3.9934(1)$ Å and $c = 4.0348(1)$ Å. These data are also comparable to the values $a = 3.996(2)$ Å, $c = 4.036(3)$ Å reported by Zhou *et al.* (33), and the values $a = 3.994$ Å, $c = 4.038$ Å reported in JCPDS (No. 5-626).

The samples BLTC10 to BLTC11 (corresponding to $Ba_{1-x}La_xTi_{1-x}Cr_xO_3$ with $x = 0.030$, 0.035) consist of a tetragonal solid solution phase $Ba_{1-t}La_tTi_{1-t}Cr_tO_3$ and a cubic solid solution phase $Ba_{1-c1}La_{c1}Ti_{1-c1}Cr_{c1}O_3$. The lattice parameters of the tetragonal phase $Ba_{1-t}La_tTi_{1-t}Cr_tO_3$ are shown in Fig. 3. According to Eqs. [1] and [2], t is suggested to be about 0.029. Therefore, the present work suggests that the tetragonal solid solution $Ba_{1-x}La_xTi_{1-x}Cr_xO_3$ exists in the range $0 \le x \le 0.029$.

3.2. Cubic Solid Solution

The samples BLTC12 to BLTC24 (corresponding to $Ba_{1-x}La_xTi_{1-x}Cr_xO_3$ with $x = 0.04$, 0.05, 0.06, 0.08, 0.10, 0.20, 0.40, 0.50, 0.52, 0.54, 0.56, 0.58, 0.60) are found to be single-phase samples with the same structure as cubic $BaTiO_3$. Table 2 lists the corresponding lattice parameters. The space group for them is $Pm\bar{3}m$. Ba and La are at the 1*a* site, (0, 0, 0); Ti and Cr at the 1*b* site, (0.5, 0.5, 0.5); O at the 3*c* site, (0, 0.5, 0.5). Figure 4 shows a typical powder X-ray diffraction pattern of the sample BLTC18 ($Ba_{1-x}La_xTi_{1-x}Cr_xO_3$ with $x = 0.40$) and the corresponding fitting pattern with GSAS.

The lattice parameter, a, decreases with increasing doping, as shown in Fig. 5. It is found that this decrease follows the equation below:

$$a_{cx} = a_{c0}(1 - x) + a_{c1}x. \qquad [3]$$

Here, x is the ratio of La/(La + Ba) in the different samples, a_{cx} is the lattice parameter a of the cubic phase

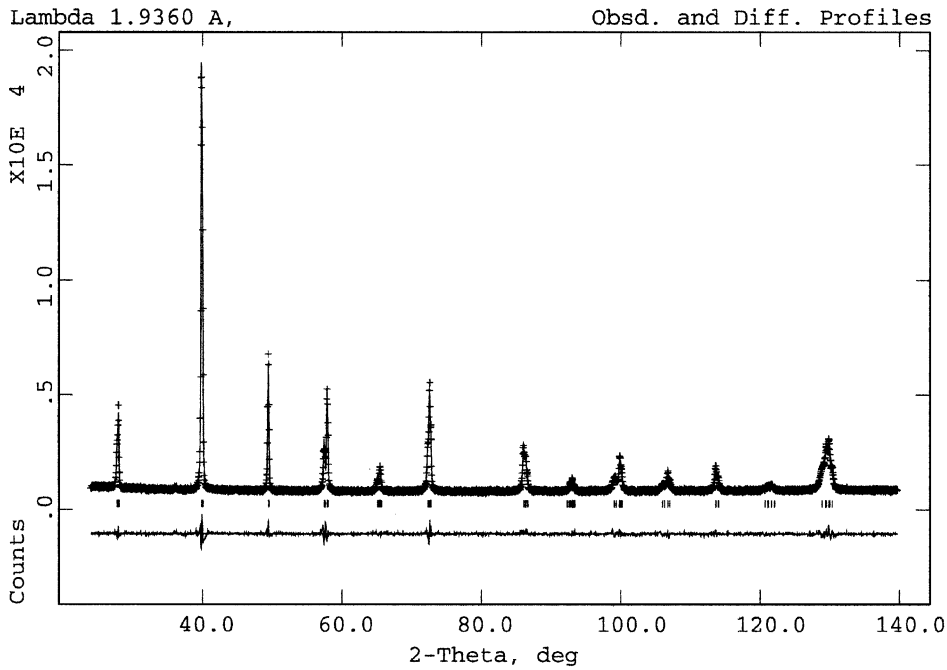

FIG. 2. Observed X-ray diffraction pattern of the sample BLTC05 and the fitted pattern using the space group *P4mm* with $R_p = 3.5\%$, $R_{wp} = 4.6\%$.

$Ba_{1-x}La_xTi_{1-x}Cr_xO_3$, a_{c0} is the expected lattice parameter a of cubic $BaTiO_3$ at room temperature, and a_{c1} is the expected lattice parameter a of the supposed cubic $LaCrO_3$. The data fit Eq. [3] very well by using $a_{c0} = 4.0006$ Å and $a_{c1} = 3.8740$ Å.

The samples BLTC10 and BLTC11 (corresponding to $Ba_{1-x}La_xTi_{1-x}Cr_xO_3$ with $x = 0.030$, 0.035) are found to be two-phase samples. They consist of a tetragonal solid solution phase $Ba_{1-t}La_tTi_{1-t}Cr_tO_3$ and a cubic solid solution phase $Ba_{1-c1}La_{c1}Ti_{1-c1}Cr_{c1}O_3$.

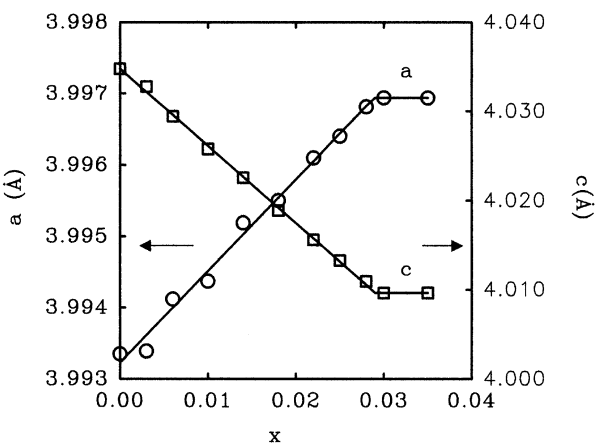

FIG. 3. Dependence of the lattice parameters a and c of the tetragonal solid solutions on the nominal composition of the samples.

The samples BLTC25 to BLTC28 (corresponding to $Ba_{1-x}La_xTi_{1-x}Cr_xO_3$ with $x = 0.62$, 0.64, 0.66, 0.68) are believed to consist of two phases, a cubic solid solution $Ba_{1-c2}La_{c2}Ti_{1-c2}Cr_{c2}O_3$ and a rhombohedral solid solution $Ba_{1-r1}La_{r1}Ti_{1-r1}Cr_{r1}O_3$.

TABLE 2
Lattice Parameter a of the Cubic Phase in the Series $Ba_{1-x}La_xTi_{1-x}Cr_xO_3$

Sample	x	a (Å)
BLTC10	0.030	3.9960(1)
BLTC11	0.035	3.9960(1)
BLTC12	0.040	3.9956(1)
BLTC13	0.050	3.9944(1)
BLTC14	0.060	3.9931(1)
BLTC15	0.080	3.9907(1)
BLTC16	0.100	3.9880(1)
BLTC17	0.200	3.9752(1)
BLTC18	0.400	3.9497(1)
BLTC19	0.500	3.9373(1)
BLTC20	0.520	3.9348(1)
BLTC21	0.540	3.9321(1)
BLTC22	0.560	3.9297(1)
BLTC23	0.580	3.9271(1)
BLTC24	0.600	3.9248(1)
BLTC25	0.620	3.9248(1)
BLTC26	0.640	3.9248(1)
BLTC27	0.660	3.9248(1)
BLTC28	0.680	3.9248(1)

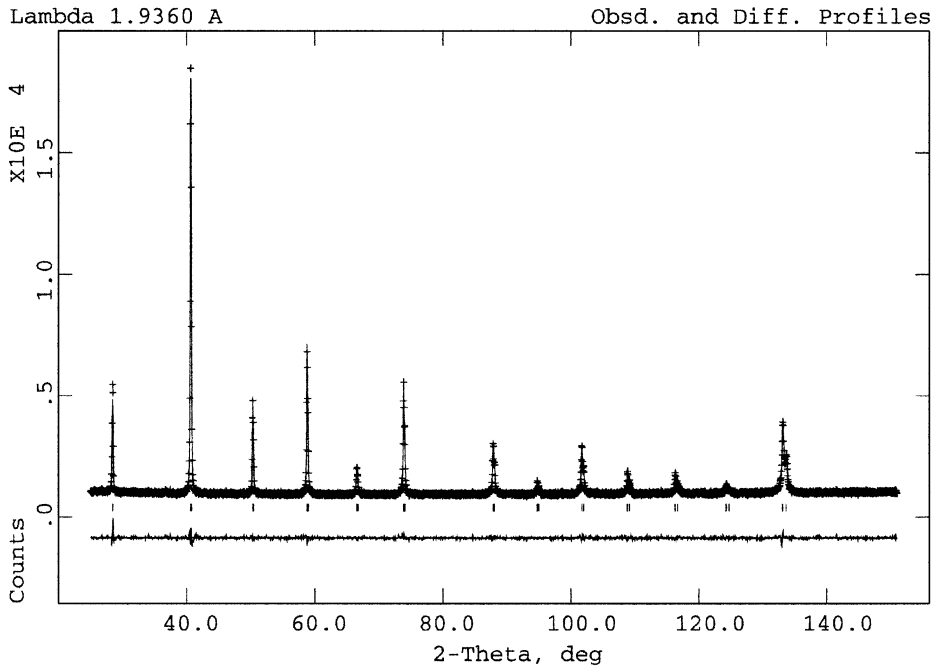

FIG. 4. Observed X-ray diffraction pattern of the sample BLTC14 and the fitted pattern using the space group $Pm\bar{3}m$ with $R_p = 2.8\%$, $R_{wp} = 3.6\%$.

Using Eq. [3] and the data from BLTC10 to BLTC11 and BLTC25 to BLTC28, the values of $c1$ and $c2$ are expected to be 0.0365 and 0.600. Therefore, the present work suggests that the cubic solid solution $Ba_{1-x}La_xTi_{1-x}Cr_xO_3$ exists in the range $0.0365 \leq x \leq 0.600$.

3.3. Rhombohedral Solid Solution

The samples BLTC29 to BLTC35 (corresponding to $Ba_{1-x}La_xTi_{1-x}Cr_xO_3$ with $x = 0.70$, 0.74, 0.78, 0.80, 0.82, 0.84, 0.86) have the rhombohedral symmetry, which is similar to $LaAlO_3$ (34). The space group is $R\bar{3}c$. Ba and La atoms are at (0, 0, 0.25), Ti and Cr atoms at (0, 0, 0), and O atoms at (0.5208, 0, 0.25). The corresponding lattice parameters are listed in Table 3. To our knowledge, this is the first to report of the existence of the rhombohedral phase $Ba_{1-x}La_xTi_{1-x}Cr_xO_3$. Therefore, typical powder

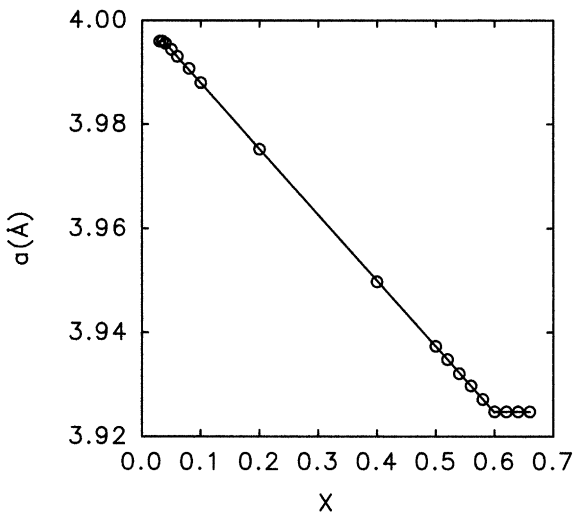

FIG. 5. Dependence of the lattice parameter a of the cubic solid solutions on the nominal composition of the samples.

TABLE 3
Lattice Parameters of the Rhombohedral Phase in the Series $Ba_{1-x}La_xTi_{1-x}Cr_xO_3$

		Hexagonal		Rhombohedral	
Sample	x	a_h (Å)	c_h (Å)	a_r (Å)	α (°)
BLTC40	0.950	5.5267(1)	13.3995(3)	3.8947(1)	90.390(1)
BLTC39	0.940	5.5267(1)	13.3995(3)	3.8947(1)	90.390(1)
BLTC38	0.930	5.5267(1)	13.3995(3)	3.8947(1)	90.390(1)
BLTC37	0.900	5.5267(1)	13.3995(3)	3.8947(1)	90.390(1)
BLTC36	0.880	5.5267(1)	13.3995(3)	3.8947(1)	90.390(1)
BLTC35	0.860	5.5273(1)	13.4116(3)	3.8962(1)	90.360(1)
BLTC34	0.840	5.5295(1)	13.4277(3)	3.8987(1)	90.330(1)
BLTC33	0.820	5.5314(1)	13.4436(3)	3.9012(1)	90.298(1)
BLTC32	0.800	5.5329(1)	13.4598(3)	3.9034(1)	90.262(1)
BLTC31	0.780	5.5345(1)	13.4733(3)	3.9055(1)	90.235(1)
BLTC30	0.740	5.5379(1)	13.5056(5)	3.9102(1)	90.168(1)
BLTC29	0.700	5.5419(1)	13.5388(5)	3.9153(1)	90.102(1)
BLTC28	0.680	5.5419(1)	13.5388(5)	3.9153(1)	90.102(1)
BLTC27	0.660	5.5419(1)	13.5388(5)	3.9153(1)	90.102(1)
BLTC26	0.640	5.5419(1)	13.5388(5)	3.9153(1)	90.102(1)
BLTC25	0.620	5.5419(1)	13.5388(5)	3.9153(1)	90.102(1)

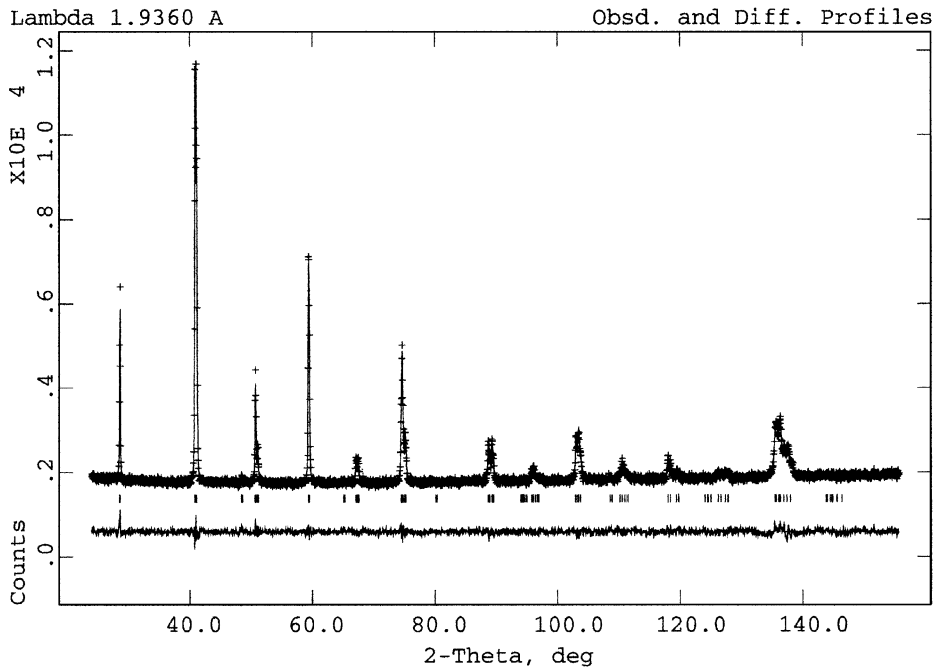

FIG. 6. Observed X-ray diffraction pattern of the sample BLTC33 and the fitted pattern using the space group $R\bar{3}c$ with $R_p = 2.0\%$, $R_{wp} = 2.6\%$.

X-ray diffraction data are presented in Table 4 for the rhombohedral phase $Ba_{1-x}La_xTi_{1-x}Cr_xO_3$ ($x = 0.82$). Figure 6 shows its powder X-ray diffraction patterns with the corresponding fitting patterns. Of course, this pattern can also be included in the $R3m$ space group, but the rhombohedral phase $Ba_{1-x}La_xTi_{1-x}Cr_xO_3$ is not a ferroelectric phase.

The lattice parameters linearly decrease with increasing x in $Ba_{1-x}La_xTi_{1-x}Cr_xO_3$, as shown in Fig. 7. The relationship between the lattice parameters and the ionic radii is very simple for the rhombohedral lattice, as shown in Fig. 8.

The following equation is found to fit the lattice parameters very well:

$$a_{Rx} = a_{R0}x + a_{R1}(1 - x). \quad [4]$$

Here, x is the ratio of La/(La + Ba) in the different samples, a_{Rx} is the lattice parameter a of the rhombohedral phase $Ba_{1-x}La_xTi_{1-x}Cr_xO_3$, a_{R0} is the expected lattice parameter a of the supposed rhombohedral $BaTiO_3$ at

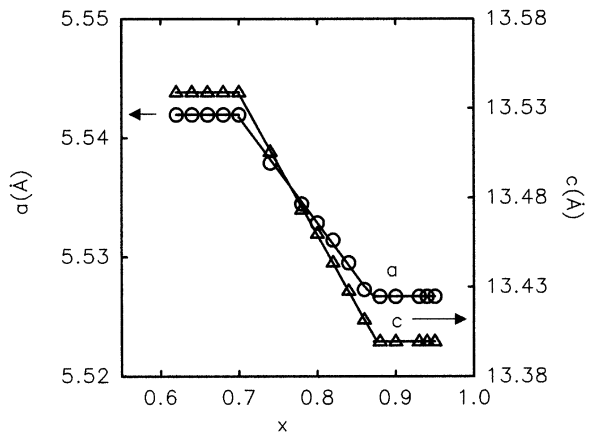

FIG. 7. Dependence of the hexagonal lattice parameters a and c of the rhombohedral solid solutions on the nominal composition of the samples.

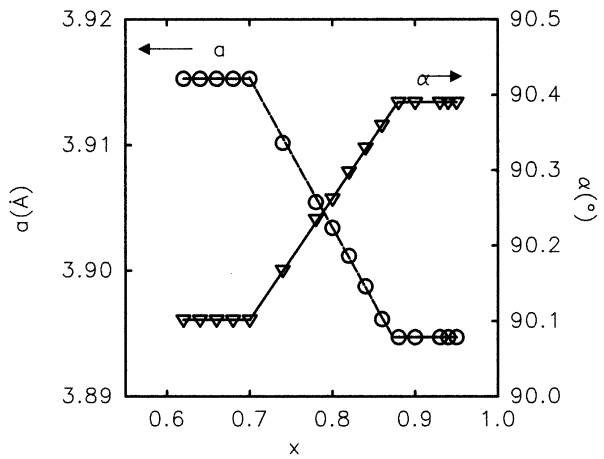

FIG. 8. Dependence of the rhombohedral lattice parameters a and α of the rhombohedral solid solutions on the nominal composition of the samples.

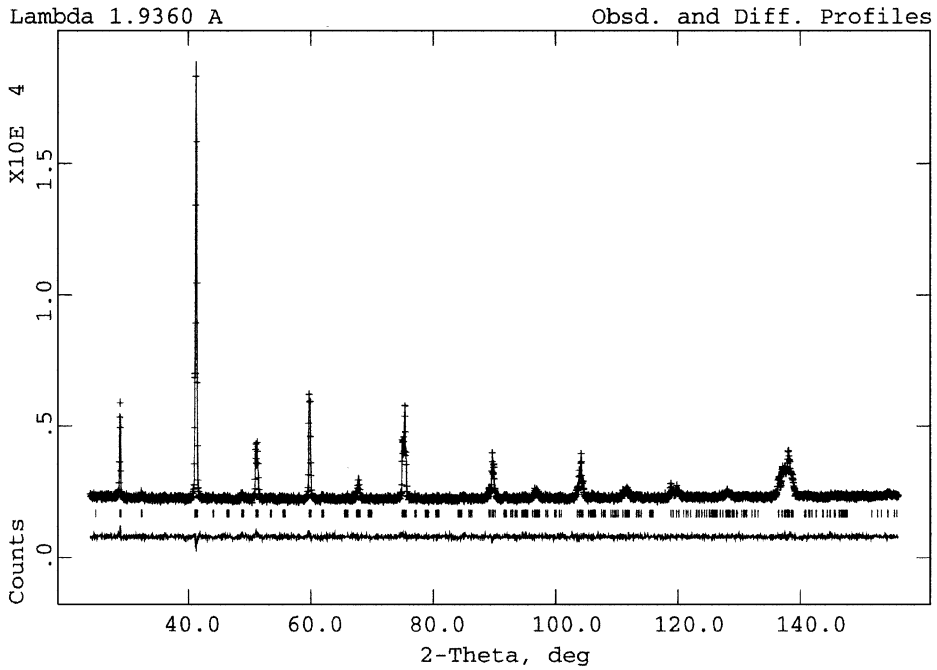

FIG. 9. Observed X-ray diffraction pattern of the sample BLTC43 and the fitted pattern using the space group *Pnma* with $R_p = 1.7\%$, $R_{wp} = 2.2\%$.

room temperature ($a_{R0} = 3.988$ Å), and a_{R1} is the expected lattice parameter a of the supposed rhombohedral $LaCrO_3$ ($a_{R1} = 3.8796$ Å).

The samples BLTC36 to BLTC40 (corresponding to $Ba_{1-x}La_xTi_{1-x}Cr_xO_3$ with $x = 0.88, 0.90, 0.93, 0.94, 0.95$) consist of two phases. These two phases are the rhombohedral solid solution $Ba_{1-r2}La_{r2}Ti_{1-r2}Cr_{r2}O_3$ and the orthorhombic solid solution $Ba_{1-o1}La_{o1}Ti_{1-o1}Cr_{o1}O_3$. Using Eq. [4] and the obtained lattice parameters, $r1$ and $r2$ are found to be 0.700 and 0.873, suggesting that the rhombohedral solid solution $Ba_{1-x}La_xTi_{1-x}Cr_xO_3$ exists in the range $0.700 \leq x \leq 0.873$.

3.4. Orthorhombic Solid Solution

The samples BLTC41 to BLTC44 (corresponding to $Ba_{1-x}La_xTi_{1-x}Cr_xO_3$ with $x = 0.96, 0.97, 0.98, 1.00$) are of a single phase with the same orthorhombic structure as $LaCrO_3$ (35–37) with $R_p \approx 1.9\%$, $R_{wp} \approx 2.4\%$ for all of these samples. The corresponding data are shown in Fig. 9 and Table 5. Figure 10 shows the typical powder X-ray diffraction pattern of the sample BLTC43 and the corresponding fit with GSAS.

The lattice parameters a, b, and c increase linearly with increasing Ba and Ti, which fulfills Vegard's law (31, 32):

$$a_{Ox} = a_{O0}x + a_{O1}(1 - x) \quad [5]$$

$$b_{Ox} = b_{O0}x + b_{O1}(1 - x) \quad [6]$$

$$c_{Ox} = c_{O0}x + c_{O1}(1 - x). \quad [7]$$

Here, x is the ratio of La/(La + Ba) in the different samples, a_{Ox}, b_{Ox}, and c_{Ox} are the lattice parameters a, b, and c of the orthorhombic phase $Ba_{1-x}La_xTi_{1-x}Cr_xO_3$, a_{O0}, b_{O0}, and c_{O0} are the expected lattice parameters a, b, and c of the supposed orthorhombic $BaTiO_3$ at room temperature ($a_{O0} = 5.5228$ Å, $b_{O0} = 7.997$ Å, and $c_{O0} = 5.6828$ Å), and a_{O1}, b_{O1}, and c_{O1} are the lattice parameters a, b, and c of the orthorhombic $LaCrO_3$ ($a_{O1} = 5.4803$ Å, $b_{O1} = 7.7599$ Å, and $c_{O1} = 5.5168$ Å).

The solution limit $o1$ of the orthorhombic solid solutions $Ba_{1-x}La_xTi_{1-x}Cr_xO_3$ is 0.956 using Eqs. [5]–[7] and the

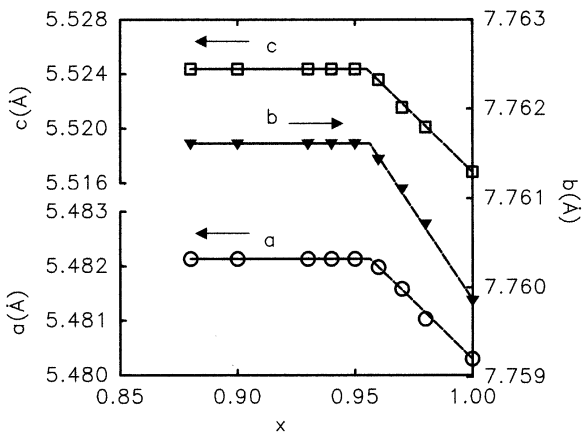

FIG. 10. Dependence of the lattice parameters a, b, and c of the orthorhombic solid solutions on the nominal composition of the samples.

TABLE 4
X-ray Diffraction Data for Rhombohedral $Ba_{1-x}La_xTi_{1-x}Cr_xO_3$ ($x = 0.82$) (20°C, $R\bar{3}c$, $a = 5.5314(1)$ Å, $c = 13.4436(1)$ Å, Fe $K\alpha$ radiation ($\lambda_{FeK\alpha1} = 1.93604$ Å) with a Mn Filter)

No.	h	k	l	$2\theta_o$	$2\theta_c$	$\Delta 2\theta$	d_o	I/I_0
1	1	0	2	28.741	28.735	0.006	3.9003	473
2	1	1	0	40.979	40.976	0.004	2.7655	1000
3	1	0	4	41.207	41.2	0.007	2.7509	932
4	2	0	2	50.809	50.814	−0.005	2.2564	348
5	0	0	6	51.207	51.194	0.013	2.2401	197
6	2	0	4	59.512	59.509	0.003	1.9505	649
7	2	1	2	67.236	67.243	−0.006	1.7484	187
8	1	1	6	67.569	67.562	0.007	1.7408	179
9	2	1	4	74.782	74.788	−0.006	1.5941	394
10	3	0	1	75.275	75.25	0.025	1.5852	231
11	2	2	0	88.846	88.856	−0.011	1.3830	225
12	2	2	1	89.474	89.45	0.023	1.3753	226
13	3	1	2	95.909	95.923	−0.013	1.3035	158
14	3	0	6	96.223	96.22	0.003	1.3003	166
15	3	1	4	103.155	103.157	−0.002	1.2356	236
16	2	1	8	103.623	103.612	0.011	1.2316	233
17	2	2	6	110.694	110.692	0.002	1.1768	178
18	4	0	4	118.188	118.205	−0.018	1.1282	199
19	0	0	12	119.578	119.554	0.025	1.1202	161
20	3	2	4	135.831	135.86	−0.029	1.0447	284
21	4	1	1	136.505	136.505	0	1.0422	237
22	1	1	12	137.609	137.582	0.027	1.0383	207

lattice parameters from the two-phase region. The orthorhombic solid solution $Ba_{1-x}La_xTi_{1-x}Cr_xO_3$ thus exists in the range $0.956 \le x \le 1.0$.

3.5. A Comment on the Two-Phase Regions

It must be emphasized that samples BLTC25 to BLTC28 ($x = 0.62$, 0.64, 0.66, 0.68) can also be fitted to a single rhombohedral structure with the space group $R\bar{3}c$ and $R_p \approx 2.2\%$, $R_{wp} \approx 2.8\%$. However, as shown in Fig. 11, the estimated lattice parameters departed from the linear relationship. The changes occur around $x = 0.68$. It is reasonable to believe that these changes are caused by the occurrence of an additional phase, the cubic solid solution phase $Ba_{1-x}La_xTi_{1-x}Cr_xO_3$. A two-phase model is then used to fit the powder X-ray diffraction data using GSAS with $R_p \approx 2.2\%$, $R_{wp} \approx 2.8\%$. Under this condition, these four samples are believed to consist of two phases, a cubic phase $Ba_{0.40}La_{0.60}Ti_{0.40}Cr_{0.60}O_3$ and a rhombohedral phase $Ba_{0.30}La_{0.70}Ti_{0.30}Cr_{0.70}O_3$. The same method was used to determine the solution limits of the other solid solutions.

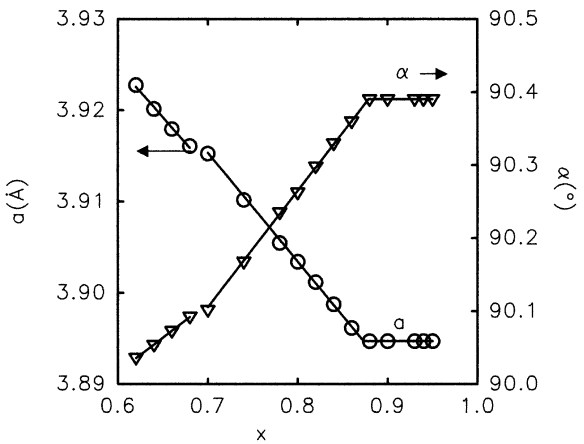

FIG. 11. Comparison of the rhombohedral lattice parameters a and α of the supposed rhombohedral phase and the real rhombohedral phase with the nominal composition of the samples.

TABLE 5
Lattice Parameters of the Orthorhombic Solid Solution $Ba_{1-x}La_xTi_{1-x}Cr_xO_3$

Name	x	a (Å)	b (Å)	c (Å)
BLTC44	1.00	5.4803(1)	7.7599(1)	5.5168(1)
BLTC43	0.98	5.4810(1)	7.7607(1)	5.5201(1)
BLTC42	0.97	5.4816(1)	7.7611(1)	5.5215(1)
BLTC41	0.96	5.4820(1)	7.7614(1)	5.5236(1)
BLTC40	0.95	5.4821(1)	7.7616(1)	5.5244(1)
BLTC39	0.94	5.4821(1)	7.7616(1)	5.5244(1)
BLTC38	0.93	5.4821(1)	7.7616(1)	5.5244(1)
BLTC37	0.90	5.4821(1)	7.7616(1)	5.5244(1)
BLTC36	0.88	5.4821(1)	7.7616(1)	5.5244(1)

4. CONCLUSION

The series $Ba_{1-x}La_xTi_{1-x}Cr_xO_3$ ($0 \le x \le 1$) has been synthesized at 1400°C in air for about 60 h and slowly cooled to room temperature. Four solid solutions can be identified in this series: tetragonal solid solution $Ba_{1-x}La_xTi_{1-x}Cr_xO_3$ ($0 \le x \le 0.029$), cubic solid solution $Ba_{1-x}La_xTi_{1-x}Cr_xO_3$ ($0.0365 \le x \le 0.600$), rhombohedral solid solution $Ba_{1-x}La_xTi_{1-x}Cr_xO_3$ ($0.700 \le x \le 0.873$), and orthorhombic solid solution $Ba_{1-x}La_xTi_{1-x}Cr_xO_3$ ($0.956 \le x \le 1$). Between the adjacent two solid solutions are the corresponding two-phase regions. The relationship between the lattice parameters and the composition of the solid solutions has been found to agree with Vegard's law (31, 32).

ACKNOWLEDGMENTS

We thank the International Exchange Office of Waseda University and Peking University for establishing the cooperative research. The support by a grant-in-aid for Research and Development of New Technology of the Association of Private Universities in Japan is gratefully acknowledged.

REFERENCES

1. G. A. Smolenski and V. A. Isupov, *Dokl. Akad. Nauk SSSR* **9,** 653 (1954).
2. G. A. Smolenskii, V. A. Isupov, A. I. Agranovskaya, and S. N. Popov, *Sov. Phys. Solid State* **2,** 2584 (1961).
3. R. M. Glaister, *J. Am. Ceram. Soc.* **43,** 348 (1960).
4. P. Gallagher, *J. Am. Ceram. Soc.* **46,** 359 (1963).
5. A. I. Kashilinski, V. I. Chechernikov, and Yu. N. Venevtsev, *Sov. Phys. Solid State* **8,** 2074 (1967).
6. I. H. Ismailzade and R. M. Ismailov, *Phys. Status Solidi A* **59,** K191 (1980).
7. M. Mahesh Kumar, M. B. Suresh, S. V. Suryanarayana, and G. S. Kumar, *J. Appl. Phys.* **84,** 6811 (1998).
8. M. Mahesh Kumar, M. B. Suresh, and S. V. Suryanarayana, *J. Appl. Phys.* **86,** 1634 (1999).
9. C. Ang, Z. Yu, and Z. Jing, *Phys. Rev. B* **61,** 957 (2000).
10. T. Mitsui and W. B. Westphal, *Phys. Rev.* **124,** 1354 (1961).
11. J. G. Bednorz and K. A. Muller, *Phys. Rev. Lett.* **52,** 2289 (1984).
12. G. I. Skanavi, I. M. Ksendzov, V. A. Trigubenko, and V. G. Prokhvatilov, *Sov. Phys. JETP* **6,** 250 (1958).
13. C. Ang, Z. Yu, P. M. Vilarinho, and J. L. Baptista, *Phys. Rev. B* **57,** 7403 (1998).
14. G. A. Smolenskii, V. A. Isupov, V. I. Agranovskaya, and S. V. Popov, *Sov. Phys. Solid State* **2,** 2584 (1967).
15. A. N. Gubkin, A. M. Kashtanova, and G. I. Skanavi, *Sov. Phys. Solid State* **3,** 807 (1961).
16. C. Ang, Z. Yu, J. Hemberger, P. Lukenheimer, and A. Loidl, *Phys. Rev. B* **59,** 6665 (1999).
17. C. Ang, Z. Yu, J. Hemberger, P. Lukenheimer, and A. Loidl, *Phys. Rev. B* **59,** 6670 (1999).
18. R. K. Dwivedi, D. Kumar, and O. Parkash, *J. Phys. D*: *Appl. Phys.* **33,** 88 (2000).
19. O. Parkash, L. Pandey, M. K. Sharma, and D. Kumar, *J. Mater. Science* **24,** 4505 (1989).
20. U. T. Hochli, K. Knorr, and A. Loidl, *Adv. Phys.* **39,** 405 (1990).
21. B. E. Vugmeister and M. D. Glinchuk, *Rev. Mod. Phys.* **62,** 993 (1990).
22. J. Toulouse, B. E. Vugmeister, and R. Pattnaik, *Phys. Rev. Lett.* **73,** 3467 (1994).
23. P. Doussineau, C. Frenois, A. Levelut, J. Toulouse, and S. Ziolkiewicz, *Ferroelectrics* **150,** 59 (1993).
24. P. Doussineau, Y. Farssi, C. Frenois, A. Levelut, K. McEnaney, J. Toulouse, and S. Ziolkiewicz, *Europhys. Lett.* **24,** 415 (1993).
25. H.-M. Christen, U. T. Hochli, A. Chatelain, and S. Ziolkiewicz, *J. Phys.: Condens. Matter* **3,** 8387 (1991).
26. G. B. Li, M. Fukunaga, Y. Uesu, and K. Kohn, *Jpn. J. Appl. Phys.* (2001), in press.
27. D. Li and M. A. Subramanian, *Solid State Sci.* **2,** 507–512 (2000).
28. H. H. Weider, *Phys. Rev.* **99,** 1161 (1955).
29. W. Merz, *Phys. Rev.* **76,** 1221 (1949).
30. J. Roth, M. Uhrmacher, P. de la Presa, L. Ziegeler, and K. P. Lieb, *Z. Naturforsch.* **55,** 242 (2000).
31. L. Vegard, *Z. Phys.* **5,** 17 (1921).
32. L. Vegard, *Z. Kristallogr.* **67,** 239 (1928).
33. L. Zhou, P. M. Vilarinho, and J. L. Baptista, *J. Am. Ceram. Soc.* **82,** 1064 (1999).
34. B. Derughetti, J. E. Drumheller, F. Laves, K. A. Muller, and F. Waldner, *Acta Crystallogr.* **18,** 557 (1965).
35. S. Geller and V. B. Bala, *Acta Crystallogr.* **9,** 1019 (1956).
36. S. Geller, *Acta Crystallogr.* **10,** 243 (1957).
37. C. P. Khattak and D. E. Cox, *Mater. Res. Bull.* **12,** 463 (1977).